# Observation of the Taylor instability in a dusty plasma

K. A. Pacha, J. R. Heinrich, S.-H. Kim, and R. L. Merlino

Citation: Phys. Plasmas **19**, 014501 (2012); doi: 10.1063/1.3671971
View online: http://dx.doi.org/10.1063/1.3671971
View Table of Contents: http://pop.aip.org/resource/1/PHPAEN/v19/i1
Published by the American Institute of Physics.

# Observation of the Taylor instability in a dusty plasma

K. A. Pacha, J. R. Heinrich, S.-H. Kim, and R. L. Merlino[a)]
*Department of Physics and Astronomy, The University of Iowa, Iowa City, Iowa 52242, USA*

(Received 20 September 2011; accepted 15 November 2011; published online 5 January 2012)

Observations of the Taylor instability in a laboratory dusty plasma are presented. The dust cloud, formed in a dc argon glow-discharge plasma, is stratified into regions of high and low dust densities. The instability was triggered by a spontaneous intrusion of the low density dust fluid into the high density dust fluid at the interface. The instability in the dust fluid was phenomenologically similar to the hydrodynamic Taylor instability that occurs when a light fluid is accelerated into a heavy fluid. © *2012 American Institute of Physics*. [doi:10.1063/1.3671971]

The Taylor instability (TI) is an instability at the interface between two fluids of different densities that occurs if the low density fluid is accelerated into the high density fluid.[1] It is a generalization of the instability, analyzed by Lord Rayleigh, that develops if a heavy fluid is superposed on a light fluid in a gravitational field.[2] The general feature of the Rayleigh-Taylor instability (RTI) is the growth of interfacial protuberances ("bubbles" and "spikes").[3] In this Brief Communication, we present observations of the TI in a dusty plasma. Dusty plasmas can exist in a broad range of states from crystalline to fluid. When the rate of momentum exchange due to dust-dust electrostatic interactions exceeds that of other interactions, a dusty plasma can be considered essentially as a one-phase (i.e., fluid) system and can be used to study hydrodynamical instabilities.[4] In radio frequency produced dusty (complex) plasmas, the RTI instability has been invoked to explain fluid phenomena at the boundary of a void,[5] and the breakup of the interface between streaming and non-streaming particle clouds.[6]

The observations were made in the device shown in Fig. 1. A glow discharge was formed in argon at a pressure of 140 mTorr (19 Pa) by applying a +300 V bias (discharge current = 23 mA) to a 3.6 cm diameter anode disk with respect to the grounded walls of a cylindrical (0.6 m diameter by 1 m length) vacuum chamber. A uniform magnetic field of 3 mT applied in the direction perpendicular to the surface of the disk confined the electrons, producing an elongated anode glow. Dust particles located on a floating tray below the anode were negatively charged, lifted upward, and confined in the anode glow.[7] Spherical iron particles, with diameters in the range of 1–5 $\mu$m were used in these experiments, although similar observations were made using dust particles composed of other materials and sizes. The dust particles were illuminated by a thin (∼mm) vertical sheet of 432 nm laser light and were imaged using a CCD camera at 30 Hz. Typical plasma and dust parameters were: electron and ion temperatures, $T_e = 100$ $T_i = 2.5$ eV, ion density, $n_i \sim 10^{14}$ m$^{-3}$, dust density, $n_d \sim 10^{10}$ m$^{-3}$, and dust charge $eZ_d \sim 2000$–10 000. Further details of the experimental set-up can be found in Ref. 8.

A single-frame image of a vertical plane through the center of the dust cloud is shown in Fig. 2(a). The dust cloud has a conical shape, with a dense region near the anode and a rarefied region farther from the anode. The image brightness was enhanced in region of low dust density (bracketed region). Fig. 2(b) shows the relative dust density profile obtained within the rectangular box in Fig. 2(a). The formation of the structured dust cloud was discussed previously.[8] The dust exhibited spontaneous vortex flows, as indicated by the arrows in Fig. 2(a). A small vortex was present at the apex of the conical cloud, with a larger vortex encompassing the entire cloud. Large scale vortex structures are common in dusty plasmas, although their cause is not fully understood.[9]

The development of the instability is shown in Fig. 3 in a montage of eight consecutive single-frame video images recorded at 1/30 s intervals. (Several examples of the instability are shown in the video in the enhanced online material.) The instability began at the location indicated by the arrow in Fig. 3(a), when a small ripple spontaneously appeared on the front side of the dense dust region. This initial perturbation grew rapidly into a wedge-shaped bubble that penetrated into the dense dust fluid [Figs. 3(b) and 3(c)]. In Fig. 3(d), a spike of dense fluid can be seen projecting back into the bubble. As the spike evolved, it rolled up into a vortex-like structure [Figs. 3(e)–3(g)] and eventually coalesced with the bubble [Fig. 3(h)]. As they developed, the bubble and spike moved upward (bottom to top in Fig. 3) at a speed ∼2–3 cm/s, within the overall flow pattern of the dust suspension shown in Fig. 2(a). When the unstable segment of the boundary moved upward, a stable boundary was restored where the instability first occurred, until it was disturbed again by the next occurrence of the instability. The recurrence time of the instability was intermittent but was generally in the range of 0.4–0.7 s.

The evolution of the bubble and spike was studied by plotting the scattered light intensity within the rectangle as shown in Fig. 3(b). The results in Fig. 4 show the penetration of the bubble (t = 0 to t = 0.2 s) into the dense dust fluid, followed at t = 0.27 s, by the appearance of a spike of dense dust fluid pushing back into the bubble (t = 0.27 s to t = 0.3 s), toward the initial unperturbed boundary. By t = 0.3 s, the spike had expanded, filling the bubble and restoring the

[a)]Electronic mail: robert-merlino@uiowa.edu.

 

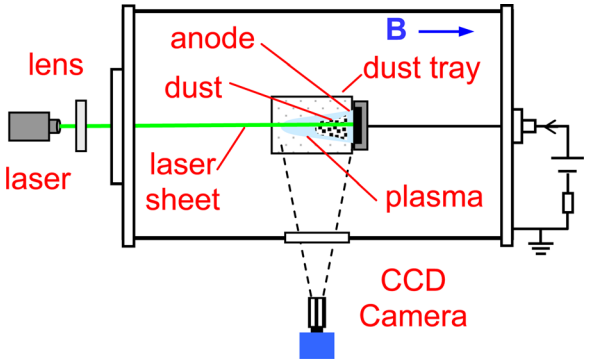


FIG. 1. (Color online) Schematic of the experimental set-up.

initial boundary. The amplitude of the instability was obtained from measurements of the area of the bubble, $A_b$, using $A_b^{1/2}$ as an indicator of the amplitude. A plot of $A_b^{1/2}$ vs. time for seven separate instability episodes is shown in Fig. 5. Although there were variations from episode to episode, each occurrence showed the same general trend of bubble formation and growth lasting about

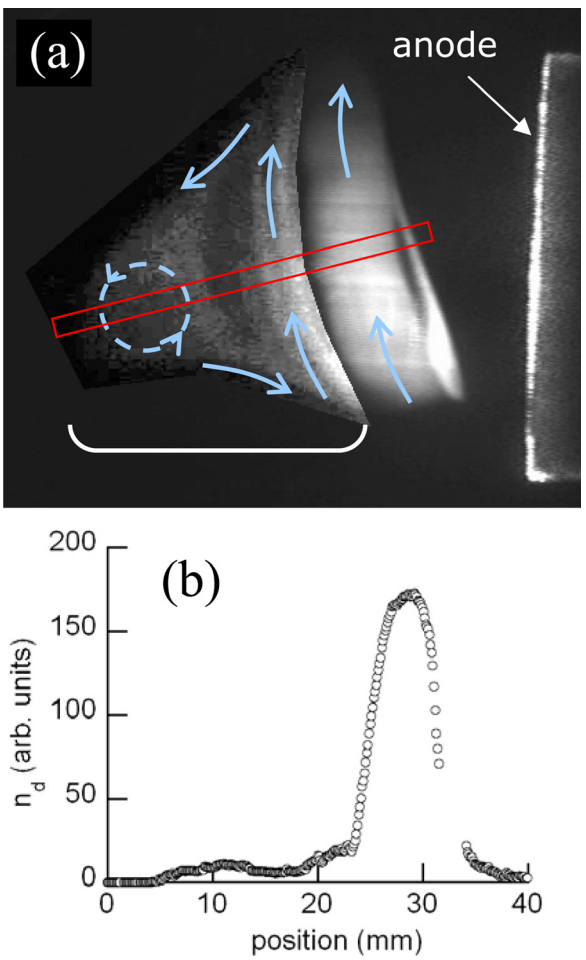


FIG. 2. (Color online) (a) Single-frame video image of the dust cloud. The image brightness in the portion of the cloud above the bracket was enhanced for ease of visualization. The arrows indicate the general direction of the vertical flow pattern in the cloud. (b) A scan of the scattered light intensity (proportional to the dust density) measured along the rectangular box in (a), showing that the suspension is stratified into low and high density regions.

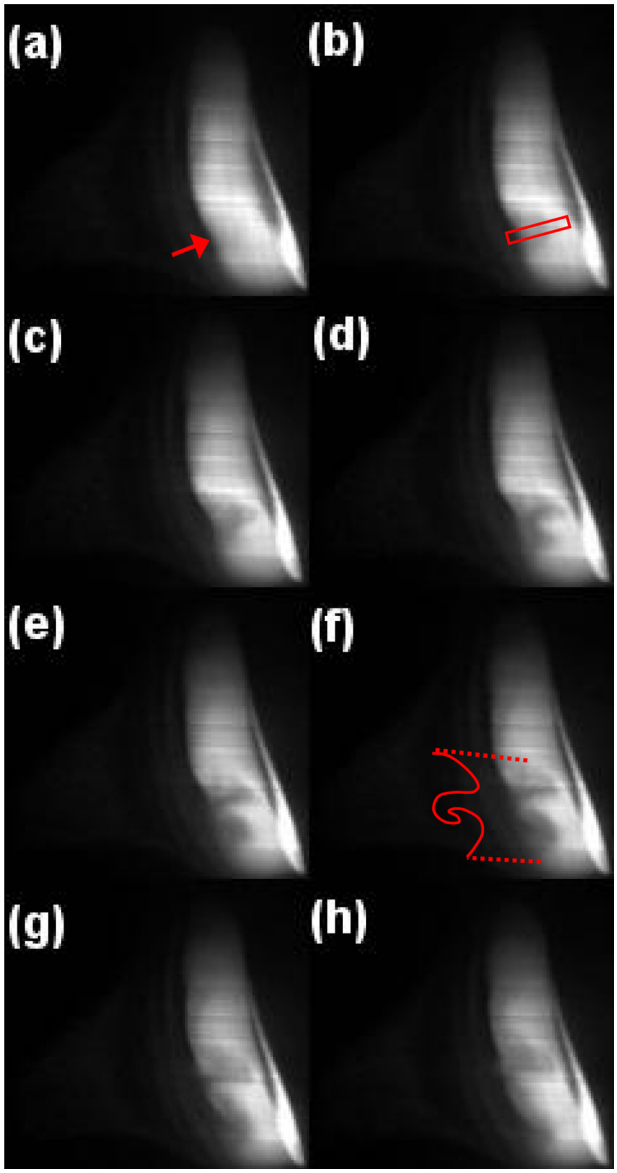


FIG. 3. (Color online) (a)–(h) Single-frame video images, in 1/30 s intervals, showing the onset and development of the instability on the interface between the low and high density dust fluids. The arrow in (a) indicated the location of the initial perturbation. (b) and (c) The growth and penetration of a bubble. (d) and (e) Growth of the spike. (f) and (g) spike roll-up (indicated by the enlarged dotted curve). (h) Merging of the bubble and spike (enhanced online). [URL: http://dx.doi.org/10.1063/1.3671971.1]

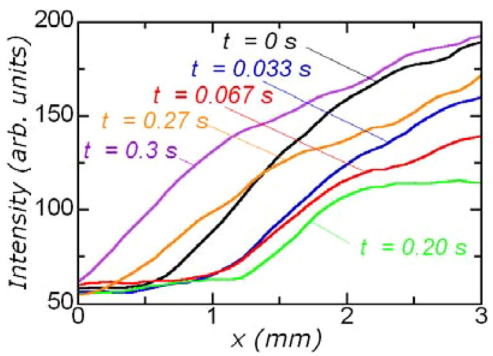


FIG. 4. (Color online) Scattered light intensity profiles for the rectangular box shown in Fig. 3(b). t = 0 refers to the initial appearance of the ripple on the interface, taken as x = 0.

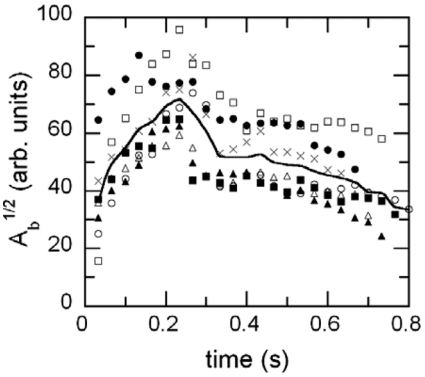


FIG. 5. Time history of the bubble amplitude, $A_b^{1/2}$, where $A_b$ is the bubble area. Different symbols refer to different occurrences of the instability

0.2 s, followed by the appearance of the spike pushing back into the bubble.

The development of the observed instability is similar to that described by Sharp[3] for a Taylor unstable interface between two *incompressible* liquids. Within a single video frame (1/30 s) of its appearance, the ripple penetrated into the dense fluid by an amount comparable with its transverse dimension (wavelength). According to linear theory,[1] the exponential growth of the instability ceases when the size of the disturbance of the interface is no longer small compared with the wavelength. The observations showed that the linear growth phase must have occurred within one video frame (1/30 s). For two semi-infinite *incompressible* fluids of mass densities $\rho_1$ and $\rho_2 > \rho_1$ separated by a planar boundary and subjected to a sinusoidal perturbation of wavelength $\lambda$, the linear growth rate is given $\gamma = \sqrt{(2\pi g'/\lambda)A_T}$, where $g'$ is the acceleration of the light fluid into the heavy fluid, $\lambda$ is the wavelength of the perturbation, and $A_T = (\rho_2 - \rho_1)/(\rho_2 + \rho_1)$ is the Atwood number.[1] From data in Figs. 2 and 4, we estimate that $g' \sim 900$ mm/s$^2$, $\lambda \sim 5$ mm, and $A_T \sim 0.8$, so that $\gamma \sim 30$ s$^{-1}$, which is consistent with the observations. The formation of the bubble and spike is an indication of the nonlinear state of the instability.[3] The roll-up of the spike could be caused by a secondary, shear-driven, Kelvin-Helmholtz instability.

The linear theory of the TI assumes that a sinusoidal perturbation is initially applied to the interface. This, however, is not the situation typically encountered in most cases of practical interest in which the nature of the initial disturbance on the interface is not known. We found that the initial disturbance always seemed to occur at roughly the same location on the interface, which could be related to the curvature of the interface. The portion of the interface where the instability appeared was flatter than at other locations. A convex surface tends to be more unstable to the TI than a concave one,[10] which might explain why the instability usually started on the flattest part of the interface.

This work was supported by DOE Grant No. DE-FG01-04ER54795.

[1]G. Taylor, Proc. R. Soc. London, Ser. A **201**, 192 (1950).
[2]L. Rayleigh, Proc. London Math Soc. **s1-14**, 170–177 (1882).
[3]D. H. Sharp, Physica **12D**, 3 (1984).
[4]G. E. Morfill, M. Rubin-Zuzic, H. Rothermel, A. V. Ivlev, B. A. Klumov, H. M. Thomas, and U. Konopka, Phys. Rev. Lett. **92**, 175004 (2004); S. A. Khrapak, A. V. Ivlev, and G. E. Morfill, Phys. Rev. E **70**, 056405 (2004).
[5]M. Schwabe, M. Rubin-Zuzic, S. Zhdanov, A. V. Ivlev, H. M. Thomas, and G. E. Morfill, Phys. Rev. Lett. **102**, 255005 (2009).
[6]R. Heidemann, S. Zhdanov, R. R, Sütterlin, H. M. Thomas, and G. E. Morfill, Europhys. Lett. **96**, 15001 (2011).
[7]T. Trottenberg, D. Block, and A. Piel, Phys. Plasmas **13**, 042105 (2006).
[8]J. R. Heinrich, S.-H. Kim, and R. L. Merlino, Phys. Rev. E **84**, 026403 (2011).
[9]G. E. Morfill, H. M. Thomas, U. Konopka, M. Zusic, A. Ivlev, and J. Goree, Phys. Rev. Lett. **83**, 1598 (1999); V. E. Fortov, O. S. Vaulina, O. F. Petrov, V. I. Molotkov, A. V. Chernyshev, A. M. Lipaev, G. Morfill, H. Thomas, H. Rotermell, S. A. Khrapak, Yu. P. Semenov, A. V. Ivanov, S. K. Krikalev, and Yu. P. Gidzenko, JETP **96**, 704 (2003); W. J. Goedheer and M. R. Akdim, Phys. Rev. E **68**, 045401 (2003); M. Rubin-Zuzic, H. M. Thomas, S. K. Zhdanovm, and G. E. Morfill, New J. Phys. **9**, 39 (2007).
[10]R. Krechetnikov, J. Fluid Mech. **625**, 387 (2009).